Geometric Analysis of Optical Frequency Conversion and its Control in Quadratic Nonlinear Media

G.G. Luther, M.S. Alber[1],
J.E. Marsden[2], J.M. Robbins
Basic Research Institute in the Mathematical Sciences
HP Laboratories Bristol
HPL-BRIMS-2000-07
6th March, 2000*

Frequency conversion and its control among three light waves is analyzed using a geometric approach that enables the dynamics of the waves to be visualised on a closed surface in three dimensions. It extends the analysis based on the undepleted-pump linearization and provides a simple way to understand the fully nonlinear dynamics. The Poincaré sphere has been used in the same way to visualise polarization dynamics. A geometric understanding of control strategies that enhance energy transfer among interacting waves is introduced, and the quasi-phase-matching strategy that uses microstructured quadratic materials is illustrated in this setting for both type-I and -II second harmonic generation, and for parametric three-wave interactions.

[1] Department of Mathematics, University of Notre Dame, Notre Dame, IN 46556
[2] Control and Dynamical Systems 107-81, Caltech, Pasadena, CA 91125
* Internal Accession Date Only
© Copyright Hewlett-Packard Company 2000

Geometric Analysis of Optical Frequency Conversion and its Control in Quadratic Nonlinear Media

G. G. Luther

The Basic Research Institute in the Mathematical Sciences (BRIMS), Hewlett-Packard Laboratories, Filton Road, Stoke Gifford, Bristol BS12 6QZ, UK

Control and Dynamical Systems 107-81, Caltech, Pasadena, CA 91125

Department of Mathematics, University of Notre Dame, Notre Dame, IN 46556

Engineering Sciences and Applied Mathematics Department, McCormick School of Engineering and Applied Science, Northwestern University, 2145 Sheridan Road, Evanston, IL 60208

M. S. Alber

Department of Mathematics, University of Notre Dame, Notre Dame, IN 46556

J. E. Marsden

Control and Dynamical Systems 107-81, Caltech, Pasadena, CA 91125

J. M. Robbins

The Basic Research Institute in the Mathematical Sciences (BRIMS), Hewlett-Packard Laboratories, Filton Road, Stoke Gifford, Bristol BS12 6QZ, UK

School of Mathematics, University Walk, Bristol BS8 1TW UK

January 29, 2000

Abstract

Frequency conversion and its control among three light waves is analyzed using a geometric approach that enables the dynamics of the waves to be visualized on a closed surface in three dimensions. It extends the analysis based on the undepleted-pump

linearization and provides a simple way to understand the fully nonlinear dynamics. The Poincaré sphere has been used in the same way to visualize polarization dynamics. A geometric understanding of control strategies that enhance energy transfer among interacting waves is introduced, and the quasi-phase-matching strategy that uses microstructured quadratic materials is illustrated in this setting for both type-I and -II second harmonic generation, and for parametric three-wave interactions.

1. INTRODUCTION

Energy conversion among light waves occurs in optical materials where the interaction of the light with the material is well characterized by expanding the polarizability up to at least second order in the electric field. Over a fixed length the conversion efficiency depends on a resonance condition among the frequencies and one among the wave numbers. Conversion efficiency also depends on the coupling strength among the waves. The magnitude of this coupling is given by the quadratic coefficient, $\chi^{(2)}$, in the amplitude expansion of the polarizability.[1–3] The dynamical evolution of three waves resonantly coupled in this way is captured by the three-wave equations for their slowly-varying envelopes. Because optical materials tend to have relatively weak nonlinear response there has been great interest in improving the effective response by microstructuring them. Here we view this as a nonlinear control problem and introduce a simple geometric picture for the dynamics and control of resonant wave interactions.

Solutions of the three-wave equations have been known in nonlinear optics almost since its inception in the early 1960's.[4] Since this early work, an extensive literature on the analysis and application of these solutions in nonlinear optics has developed. In previous investigations, the dynamics of the three-wave system was reduced with the aid of the Manley-Rowe relations to a single nonlinear oscillator.[4–8] Features of the canonical Hamiltonian structure of the three-wave system have also been exploited.[6–8] In what follows we introduce a different approach.

The present approach is based on a systematic theory of Hamiltonian systems with symmetry,[9] called *reduction*. For the three-wave equations, the symmetries are just the phase invariances associated with the Manley-Rowe relations, and the reduction procedure leads to a two-dimensional reduced phase space, the *three-wave surface*, in which the three wave amplitudes and their relative phase are incorporated simultaneously. In contrast, the standard approach reduces the three-wave system to a phase space for the modulus of a single wave amplitude.

The three-wave surfaces are deformed spheres, and the dynamics on them is described using a simple geometrical construction.[10,11] This construction provides a means of visualizing the dynamics of three-wave interactions, analogous to the use of the Poincaré sphere for polarization dynamics,[12–14] and it enables existing analysis to be readily comprehended in geometrical terms. In this way, recent techniques of geometric mechanics provide fresh insight into the dynamics of second harmonic generation and parametric frequency conversion in quadratic, or $\chi^{(2)}$, media. In particular, this geometrical treatment facilitates the analysis of the control of three-wave interactions.

As early as 1962, Armstrong, Bloembergen, Ducuing and Pershan[4] proposed that the flow of energy among interacting light waves could be controlled by modulating the sign of the susceptibility. In recent years these basic ideas have been implemented to simplify frequency conversion[15] and to improve optical parametric oscillators.[16] By formulating the dynamics in terms of the three-wave surface, we introduce a powerful and relatively simple method of analyzing control strategies for second harmonic generation and parametric frequency conversion. The analysis described below extends the standard theory of quasi-phase-matching[4,5,7,15], in which the three-wave equations are linearized using the undepleted-pump approximation. It complements the previous analysis of quasi-phase-matching that allows pump depletion,[5] by enabling a simple visual and qualitative understanding of the results without explicit analysis of elliptic integrals.

The paper is organized as follows. First we review the Hamiltonian structure of the three-wave system (Sec. 2), emphasizing the connection between the Manley-Rowe relations

and phase symmetries. These phase symmetries are then used to reduce the three-wave system to a system in three real variables X, Y, and Z, chosen to be invariant under the phase symmetries (Sec. 3). The dynamics in (X, Y, Z)-space is shown to be confined to a closed cubic surface of revolution, the three-wave surface. The trajectories are given by intersections of the three-wave surface with a family of parallel planes, whose slope measures the relative strength of the wave vector mismatch and the quadratic nonlinearity (Sec. 4). This geometric realization of the three-wave dynamics is then used to analyze techniques for controlling frequency conversion in $\chi^{(2)}$ media, and approximations are obtained when the phase mismatch dominates. Quasi-phase-matching of both type-I and type-II second-harmonic generation, as well as generic parametric three-wave interactions are described using the three-wave surface (Sec. 5).

2. THE THREE-WAVE EQUATIONS AND THEIR SYMMETRIES

The three-wave equations, written

$$\frac{dA_1}{dz} = -i\gamma_1 A_2^* A_3 \exp(-i\Delta k z) \ , \tag{1a}$$

$$\frac{dA_2}{dz} = -i\gamma_2 A_1^* A_3 \exp(-i\Delta k z) \ , \tag{1b}$$

$$\frac{dA_3}{dz} = -i\gamma_3 A_1 A_2 \exp(i\Delta k z) \ , \tag{1c}$$

are obtained as a slowly-varying amplitude approximation of Maxwell's equations for the resonant interaction of three light waves propagating in a non-centrosymmetric material.[4] Here the A_j are the slowly-varying envelopes, and each has a different carrier frequency. The choice of the γ_j defines the optical interaction as well as the units or normalization of the complex amplitudes. The amplitudes are typically related to units of power or intensity both in the literature[4] and in texts on nonlinear optics.[1,2]

Both second harmonic generation and parametric frequency conversion are modeled by the three-wave equations, where each A_j is a complex light-wave amplitude, $\Delta k = k_1 + k_2 - k_3$ is the wave-vector mismatch, and each γ_j is proportional to the second-order susceptibility,

$\chi^{(2)}$ of the process. For type-II second harmonic generation, waves one and two, having the same frequency, propagate in different polarization states and interact to generate a third light wave at the second harmonic frequency. In the limit $A_1 = A_2$ and $\gamma_1 = \gamma_2$ the equations for type-I second harmonic generation are obtained. If this condition is true for the initial conditions, it continues to be the case for all time. Thus, the condition is dynamically invariant, and type-I second harmonic generation is always a special case of the three-wave system.

In what follows it is convenient to shift into a rotating frame and rescale the wave amplitudes by making the transformation $A_j = |\gamma_j| q_j \exp(-i\Delta k z)$, so that the three-wave equations become

$$\frac{dq_1}{d\xi} = i\Delta\Gamma q_1 - isq_2^* q_3 \ , \tag{2a}$$

$$\frac{dq_2}{d\xi} = i\Delta\Gamma q_2 - isq_1^* q_3 \ , \tag{2b}$$

$$\frac{dq_3}{d\xi} = i\Delta\Gamma q_3 - isq_1 q_2 \ , \tag{2c}$$

where $\xi = z\sqrt{|\gamma_1\gamma_2\gamma_3|}$ is the scaled propagation length, and $\Delta\Gamma = \Delta k/\sqrt{|\gamma_1\gamma_2\gamma_3|}$ is the relative strength of the mismatch compared to the nonlinearity. Here $s = \pm 1$ is the sign of the coefficient of the quadratic nonlinearity. Notice that along with the initial data, solutions of this system depend only on the parameters $\Delta\Gamma$ and s. The parameter $\Delta\Gamma$ plays a crucial role in determining the qualitative dynamics. The parameter s models the reversal of the crystal orientation, and it will be used in the analysis of quasi-phase-matching. Written in this form the three-wave system has the canonical Hamiltonian structure

$$\frac{dq_j}{dz} = \{q_j, H\} = -2i\frac{\partial H}{\partial q_j^*} \ , \tag{3}$$

where the Hamiltonian,

$$H = \frac{s}{2}(q_1^* q_2^* q_3 + q_1 q_2 q_3^*) - \frac{\Delta\Gamma}{2}\sum_{j=1}^{3} |q_j|^2 \ , \tag{4}$$

is cubic in the wave amplitudes. The Poisson bracket $\{,\}$ produces

$$\{q_i, q_j\} = 0 \ , \tag{5a}$$

$$\{q_i, q_j^*\} = -2i\delta_{ij} \ . \tag{5b}$$

In addition to the Hamiltonian itself, the Manley-Rowe relations

$$K_1 = \frac{1}{2}\left(|q_1|^2 - |q_2|^2\right) \ , \tag{6a}$$

$$K_2 = \frac{1}{2}\left(|q_2|^2 + |q_3|^2\right) \ , \tag{6b}$$

$$K_3 = \frac{1}{2}\left(|q_1|^2 + |q_3|^2\right) \ , \tag{6c}$$

are constants of the motion. Since any two K_j along with H form a complete and independent set of conserved quantities, ie $\{K_i, K_j\} = 0$ and $\{K_i, H\} = 0$, the system can be solved and solutions expressed in terms of elliptic integrals. This procedure is usually carried out by transforming the complex envelope amplitudes to real coordinates ρ_j, ϕ_j defined by $q_j = \rho_j^\beta \exp(i\phi_j)$, where β may be either 1 or 1/2. Using the Manley-Rowe invariants (6a)-(6c), the system is reduced to a one degree of freedom potential equation and then to quadratures by eliminating the dependence on each of the other variables.[4,5,7,6,8]

Analysis of this nonlinear oscillator and the associated elliptic integrals then provides information about the dynamics of the system. The phases may also be studied in terms of integrals of elliptic functions.[17,18]

Notice that this procedure reduces the three-wave phase space to that of a one-dimensional nonlinear oscillator. Unfortunately, only information about a single wave amplitude (and indirectly the relative phase) of the system is retained in this representation. By exploiting the fact that the Manley-Rowe invariants correspond to symmetries of the three-wave system, the three-wave phase space is reduced to a closed two-dimensional surface in three-dimensions. This representation of the dynamics retains information about all of the amplitudes and the relative phase.

The phase space coordinates are chosen to be invariant with respect to symmetries connected to the Manley-Rowe invariants (6a)-(6c). These symmetries manifest themselves in

the three-wave equations as invariants with respect to phase shifts. One way to understand this is to let each of the K_j act as the "Hamiltonian" in the canonical equations of motion (3). The dynamics generated by each K_j introduces phase shifts, a unitary transformation, on the vector of three-wave amplitudes. In real coordinates $q_j = x + iy$ these are just the motions of uncoupled harmonic oscillators. The specific phase shifts associated with the Manley-Rowe symmetries are

$$(q_1, q_2, q_3) \to (q_1 \exp(-i\theta_1), q_2 \exp(i\theta_1), q_3), \tag{7a}$$

$$(q_1, q_2, q_3) \to (q_1, q_2 \exp(-i\theta_2), q_3 \exp(-i\theta_2)), \tag{7b}$$

$$(q_1, q_2, q_3) \to (q_1 \exp(-i\theta_3), q_2, q_3 \exp(-i\theta_3)) \ , \tag{7c}$$

for K_1 through K_3, respectively. It is easily checked that the three-wave equations (2a)–(2c) are invariant under these transformations.

3. REDUCTION TO THREE-WAVE SURFACES

If a system of first-order ordinary differential equations has a phase symmetry, its dimension can be reduced by one by ignoring the value of the phase in question. If the system is Hamiltonian, its dimension can be reduced by two; associated to the phase symmetry is a conserved quantity, and fixing its value eliminates an additional degree of freedom. The theory of reduction generalizes this procedure in a systematic way.[9]

Projection of polarization dynamics onto the Poincaré sphere is a simple example of reduction. The dynamics of the two polarization components are modeled by two coupled complex amplitude equations. There are typically no frequency mixing terms, but the equations conserve the total intensity. Since the equations are Hamiltonian, intensity conservation reduces the dimension of the system from four to two. This conserved quantity is also associated with a phase symmetry of the equations. The Stokes parameters[12] are invariant coordinates with respect to this phase symmetry that project the dynamics onto the Poincaré sphere. The dynamics of the amplitudes and the relative phase of the polarization

components is retained in the reduced phase space, but the absolute phase is not. In the following analysis reduction is applied to three-wave interactions.

Reduction of the three-wave system is achieved by introducing new coordinates that are invariant with respect to the phase symmetries (7a)–(7c) associated with the Manley-Rowe relations. As noted above, only two of these symmetries are independent. Since the three-wave system has three complex, or six real, dimensions, it follows that there are four independent phase-invariant coordinates. The coordinates (X, Y, Z) defined by

$$X + iY = q_1 q_2 q_3^* \ , \tag{8a}$$

$$Z = \sum_{j=1}^{3} p_j |q_j|^2 \ , \tag{8b}$$

where the p_j are real constants, are clearly invariant under the phase symmetries, as are the associated conserved quantities K_1, K_2 and K_3 of the Manley-Rowe relations. Thus we expect two relations amongst the invariants X, Y, Z and K_1, K_2, K_3. We have already noted the relation $K_3 = K_1 + K_2$. The second relation is obtained by taking the square modulus of $X + iY$ and expressing the $|q_j|^2$ that come from the right hand side of (8a) in terms of Z and the Manley-Rowe relations. This yields the relation $\phi = 0$, where

$$\phi = -\eta(X^2 + Y^2) + \kappa(Z - Z_1)(Z + Z_2)(Z - Z_3) \ , \tag{9}$$

$$\kappa = 1/\eta^2, \quad Z_1 = 2(p_3 K_2 + p_1 K_1), \quad Z_2 = 2(p_1 K_3 + p_2 K_2) \quad \text{and} \quad Z_3 = -2(p_2 K_1 - p_3 K_3),$$

and $\eta = p_1 + p_2 - p_3$.

The function $\phi = 0$ implicitly defines for given K_1, K_2 and K_3 the three-wave surface in (X, Y, Z)-space. Since the K_j are also constants of the motion, the three-wave dynamics is captured by the motion dynamics of (X, Y, Z). The coordinate Z can be chosen to provide a convenient comparison among intensities of the three waves. For second harmonic generation, one might choose $p = (-1, -1, 1)$, so Z provides a measure of the conversion efficiency. More light at the second harmonic corresponds to larger values of Z. By making the new coordinates invariant with respect to the Manley-Rowe phase symmetries, we have

removed information about the absolute phases of each wave. The new coordinates (X, Y, Z) include information only about the amplitudes and the relative phase among the waves.

Comparing to the standard variable transformation $q_j = \rho_j^\beta \exp(i\phi_j)$, the coordinates X and Y may be regarded as the components of a vector of length $|\rho_1\rho_2\rho_3|^\beta$ and polar angle $\Omega = (\phi_1 + \phi_2 - \phi_3)$, where Ω is the relative phase of the three waves. If $p_j = 1$ is chosen for any one value of j and $p_j = 0$ is chosen for the each of the other two values of j then $Z = \rho_j^{2\beta}$. This choice of Z provides a direct connection to the standard analysis in the case of a depleted pump.

Using the invariant coordinates X, Y and Z defined in (8a)-(8b), the three-wave system and its Hamiltonian structure can be rewritten. The reduced equations of motion can be obtained by differentiating the expressions for (X, Y, Z) in (8a)-(8b) and removing all instances of q_j by substitution. It is often more convenient to transform the equations written in terms of Poisson brackets (3). Using the reduced coordinates, the Poisson structure of the three-wave system becomes

$$\frac{dW_j}{d\xi} = \{W_j, H_r\} \ , \quad j = 1, 2, 3 \ , \tag{10}$$

where $W = (X, Y, Z)$ and H_r is the Hamiltonian (4) written using the reduced coordinates. The reduced equations of motion are obtained once the reduced Hamiltonian and Poisson brackets among the reduced coordinates are known. By direct substitution using (8a)-(8b), the reduced Hamiltonian

$$H_r = sX - \frac{\Delta\Gamma}{2\eta}(Z + 2\delta) \tag{11}$$

is obtained, where, as above, $\eta = p_1 + p_2 - p_3$ and $\delta = (p_2 - p_1)K_1 + (p_2 - p_3)K_2 + (p_1 - p_3)K_3$. This choice of coordinates leads to the important simplification that the reduced Hamiltonian is linear in X and Z and independent of Y. The reduced Poisson brackets,

$$\{X, Y\} = -\partial\phi/\partial Z \ , \tag{12a}$$

$$\{Z, X\} = -2\eta Y \ , \tag{12b}$$

$$\{Y, Z\} = -2\eta X \ , \tag{12c}$$

are obtained by computing the brackets (5a)-(5b) among the invariant coordinates (X, Y, Z). Using these results the reduced three-wave equations are written explicitly as

$$\frac{dX}{d\xi} = -\Delta\Gamma Y \tag{13a}$$

$$\frac{dY}{d\xi} = \Delta\Gamma X + s\frac{\partial\phi}{\partial Z} \tag{13b}$$

$$\frac{dZ}{d\xi} = -2s\eta Y \ . \tag{13c}$$

In this form it is clear that the coupling between X and Y is equivalent to that of a harmonic oscillator with frequency $\Delta\Gamma$, and the coupling between Y and Z is equivalent to a nonlinear oscillator. These equations can also be written in the compact form

$$\frac{dW}{d\xi} = \nabla_r H_r \times \nabla_r \phi \ , \tag{14}$$

where the gradient is taken with respect to the reduced coordinates as $\nabla_r = (\partial/\partial X, \partial/\partial Y, \partial/\partial Z)$. Since $dH_r/d\xi = \nabla_r H_r \cdot dW/d\xi$ and $d\phi/d\xi = \nabla_r \phi \cdot dW/d\xi$, it is clear from (14) that H_r and ϕ are constants of the motion.

The reduced equations (13a)–(13c) are integrated by differentiating (13c) with respect to ξ and substituting (13b). The result is a potential equation for Z

$$\frac{1}{2}\left(\frac{dZ}{d\xi}\right)^2 + U = E \tag{15}$$

where the reduced Hamiltonian, H_r, has been used to replace X, and the "energy" E is the constant of integration. The potential, U, is given by

$$U = 2\eta\left[\phi(X=0, Y=0, Z) + rZ\right] + \frac{1}{2}\Delta\Gamma^2 Z^2 \ , \tag{16}$$

where $r = \Delta\Gamma H_r + \Delta\Gamma^2\delta/2\eta$. Integrating the potential equation it is found that

$$\xi - \xi_0 = \int \frac{dZ}{\sqrt{2(E - U(Z)}} \ , \tag{17}$$

where $E - U(Z)$ is a cubic polynomial for which the sign of the coefficient of the highest power is given by the sign of η. Defining $\zeta_1 > \zeta_2 > \zeta_3$ to be real roots of $E - U(Z)$ with $\eta > 0$, then $E - U(Z) \geq 0$ on (ζ_2, ζ_3) and

$$\xi - \xi_0 = \left(\frac{2}{k}\right) \int \frac{d\theta}{\sqrt{1 - M\sin^2(\theta)}} \ , \tag{18}$$

where $M = (\zeta_2 - \zeta_3)/(\zeta_1 - \zeta_3)$ and $k = \sqrt{(\zeta_1 - \zeta_3)/2}/2$. In this case the solution is

$$Z(\xi) = \zeta_2 - (\zeta_2 - \zeta_3)\mathrm{cn}^2[\{(\zeta_1 - \zeta_2)/2\}^{1/2}(\xi - \xi_0)|M] \ , \tag{19}$$

where ζ_3 is the minimum value of Z and ζ_2 is the maximum value of Z over a period. The positions of the roots ζ_j are specified by the values of the initial data and the parameters s and $\Delta\Gamma$. This dependence is obtained by comparing the coefficients of the polynomial $E - U(Z)$ with those of its factored form. When one of the roots ζ_j can be written in terms of the extremal values of Z (and therefore the q_j) the other two are then obtained algebraically.[5,8]

The period of energy transfer among the waves is given as

$$L = \oint \frac{dZ}{\sqrt{2(E - U(Z))}} = \frac{K(M)}{k} \ , \tag{20}$$

where the loop integral is taken about neighboring roots over which $E - U(Z) \geq 0$ and $K(M)$ is the complete elliptic integral of the first kind. If Z is defined so that only one p_j is non-zero the one-dimensional potential equation obtained using the standard method with variables $\rho_j^\beta \exp(i\phi)$ is recovered. Once Z is known, the value of X is obtained using the reduced Hamiltonian, H_r, and the value of Y is then obtained using $\phi = 0$. To reconstruct the solution of the three-wave equations the wave amplitudes are then computed in terms of Z and their initial values through Manley-Rowe invariants (K_1, K_2, K_3). The relative phase is $\arg(X + iY)$. The two remaining phases are not given in terms of algebraic relations. They must be integrated. This can be done using the variables $q_j = \rho_j^\beta \exp(i\phi_j)$ and integrating $d\phi_j/d\xi$.[18,17] Recently the geometric structure of the three-wave system was exploited to obtain these phase shifts.[10] In general these shifts have a geometric and dynamic component. The geometric component is proportional to the symplectic area enclosed by an orbit on the three-wave surface.

4. THE REDUCED PHASE SPACE

The three-wave system has now been reduced to a set of equations in three space. These reduced equations produce motion confined to a closed surface in (X, Y, Z). In this section we describe how to generate the reduced phase space by constructing orbits on the three-wave surfaces. We then show how to interpret the dynamics of wave mixing in terms of motion on the reduced phase space. Recall that on these three-wave surfaces only the dynamics of the relative phase and the amplitudes of the waves are captured. In many applications the absolute phases are not needed, but they can be obtained analytically as described above.

A. GEOMETRIC CONSTRUCTION OF THE REDUCED PHASE SPACE

First recall that (14) implies H_r and ϕ are constants of the motion. Since H_r is linear, its level sets are the planes

$$Z = mX - (smH_r + 2\delta) \ , \tag{21}$$

with slopes $m = 2s\eta/\Delta\Gamma$. Expressed in terms of the wave amplitudes q_j, $\phi(X, Y, Z)$ vanishes identically. Thus the reduced dynamics is confined to the surfaces given by $\phi(X, Y, Z) = 0$. These *three-wave surfaces* are generically egg-shaped. Notice that in the case of polarization dynamics $\phi(X, Y, Z)$ is quadratic in Z and the analogous surfaces are spheres.

Trajectories of the reduced equations are the curves produced by intersecting the level sets of H_r with the three-wave surfaces. Fig. 1 shows the intersection of a three-wave surface and a planar level set of H_r. This intersection defines a trajectory of the system.

A typical reduced phase space on a three-wave surface is plotted in Fig. 2 and corresponds to either type-II second harmonic generation or parametric three-wave interactions. Apart from fixed points, the three-wave surface is filled with periodic orbits. As the system traverses one of these cycles light is converted from the pump wave to the signal and idler waves and then back to the pump wave.

Type-I second harmonic generation is realized when $K_2 = K_3$. In this limit a pair of the

roots of $\phi(X=0,Y=0,Z)=0$ coalesce, and a singular point forms. A typical phase space for type-I second harmonic generation is plotted in Fig. 3.

B. FEATURES OF THE REDUCED PHASE SPACE

The shape and size of the three-wave surface is defined by fixing the values of the Manley-Rowe invariants, which are defined by the initial values of the scaled wave amplitudes $(|q_1|,|q_2|,|q_3|)$. The plane defined by the corresponding Hamiltonian must pass through the initial point in (X,Y,Z) as defined by the initial amplitudes and phases of (q_1,q_2,q_3). The value of m then fixes the orbit associated with this initial point. After one trip around the three-wave surface, the reduced system returns to its initial position. The amplitudes and the relative phase return to their initial values.

The qualitative features of the phase space depend only on the slope m and the invariants K_j. These parameters define the interactions of the three light waves. For a fixed quadratic coefficient, m varies inversely with the phase mismatch. Near phase matching, $\Delta k \ll 1$, so $\Delta\Gamma \ll 1$ and the slope m is large, meaning the Hamiltonian planes tend to be vertical. Far from phase matching the slope m is small and the Hamiltonian planes are nearly horizontal.

The three-wave surface is always a single closed surface. For a given choice of the p_j, the K_j define the positions of the roots of $\phi(X=0,Y=0,Z)=0$. One root coincides with the top and a neighboring root coincides with the bottom of the three-wave surface. A consistent set of initial data must lie between these two roots, and all points on the trajectory that it generates must lie between the same pair of roots. This is necessary in order that X, Y and Z remain real.

An important feature which simplifies the analysis of controls is that the three-wave surfaces are independent of the value of $\Delta\Gamma$ and s, so the transformation $s \to -s$, which corresponds to changing the sign of the second order susceptibility, $\chi^{(2)}$, leaves the three-wave surface invariant.

In these calculations the vector p provides some flexibility in the definition of Z as a

linear combination of the square of the field amplitudes. In this way Z can be chosen to be proportional to the amount of conversion. For a given $\chi^{(2)}$ process the conversion efficiency can then be extracted directly from the phase portrait on the three-wave surface. If p is chosen so that the orbit passing through the highest point on the surface produces complete conversion, then for a given initial condition, m can be chosen so that the trajectory passes through the point at the top of the three-wave surface. The process of varying m is analogous to tuning the phase mismatch, Δk. Consider the choice $p = (-1, -1, 1)$. When $\Delta k = 0$, the orbit passing through $(X, Y) = (0, 0)$ produces maximum conversion.

Relative fixed points, sometimes called eigenmodes, are located at the points where the Hamiltonian planes are tangent to the three-wave surface. The value of Z remains constant at these points, so no energy is exchanged. These points are generically elliptic points. For $K_2 = K_3$, as in the case of type-I second harmonic generation, an additional relative fixed point appears at the singular point. The trajectory connected to it is homoclinic since it connects a fixed point to itself. The homoclinic trajectory, given by $H_r = 0$, divides the three-wave surface in half, with $H_r > 0$ on one side and $H_r < 0$ on the other. This orbit corresponds to the well-known tanh solution. In the phase-matched system, where $m \gg 1$, the pair of elliptic points are located on the sides of the three-wave surfaces. As m decreases and the mismatch increases, one of these points migrates toward the top and one toward the bottom. If $K_2 = K_3$ the homoclinic orbit shrinks as one of the elliptic points approaches the homoclinic point, and the portion of the phase space having characteristically nonlinear features shrinks. In the limit $m = 0$ the area enclosed by the homoclinic is zero and the motion is purely linear.

C. LINEARIZATION AND THE UNDEPLETED PUMP APPROXIMATION

In many applications the three-wave system is linearized by assuming that the pump wave remains nearly constant throughout the evolution of the wave interaction. This is always the situation near the elliptic fixed points since only small variations in the Z coordinate

occur there. As the phase mismatch becomes large compared to the strength of the nonlinear interaction, so that $\Delta\Gamma \gg 1$, the slope of the level sets of the reduced Hamiltonian H_r become small ($m \ll 1$). In this limit the Z coordinate makes small nearly sinusoidal oscillations near its initial value. This corresponds to the undepleted-pump limit.

For interactions over a single period the reduced three-wave system (13a)–(13c) can be linearized in the limit $\Delta\Gamma \gg 1$. Take $\Delta\Gamma = \Gamma/\epsilon$, where $0 < \epsilon \ll 1$. Rescale the evolution variable so $T = \xi/\epsilon$ and obtain

$$\frac{dX}{dT} = -\Gamma Y \tag{22a}$$

$$\frac{dY}{dT} = \Gamma X + s\epsilon\frac{\partial\phi}{\partial Z} \tag{22b}$$

$$\frac{dZ}{dT} = -2s\epsilon\eta Y \ . \tag{22c}$$

Now linearize by letting $W = (X, Y, Z) = W_0 + \epsilon\delta W$. To leading order in ϵ,

$$\frac{dX_0}{dT} = -\Gamma Y_0 \ , \tag{23a}$$

$$\frac{dY_0}{dT} = \Gamma X_0 \ , \tag{23b}$$

$$\frac{dZ_0}{dT} = 0 \ . \tag{23c}$$

Consistent with the undepleted-pump approximation, no conversion takes place. At this order the system simply oscillates in the (X, Y)-plane with frequency Γ. This corresponds to a period of $2l_c = 2\pi/\Delta\Gamma$. In the physical coordinates l_c is $\pi/\Delta k$. Note that when $K_2 = K_3$ special care must be taken near the homoclinic orbit, but as noted above the area enclosed by this orbit tends to zero as m tends to zero.

At the next order in ϵ, the dynamics is governed by the equations,

$$\frac{d\,\delta X}{dT} = -\Gamma\delta Y \ , \tag{24a}$$

$$\frac{d\,\delta Y}{dT} = +\Gamma\delta X + s\left.\frac{\partial\phi}{\partial Z}\right|_{Z=Z_0} \ , \tag{24b}$$

$$\frac{d\,\delta Z}{dT} = -2s\eta\,\delta Y \ . \tag{24c}$$

These equations reveal that the first correction to the oscillation in the (X, Y) plane is to shift its center along the X-direction by introducing a constant driving term determined by

the value of Z_0. In addition, there is now motion in the Z-coordinate. This motion is slaved to the rate of change of the Y-coordinate and is thus a small oscillation. As expected this gives a small amount of conversion and introduces motion perpendicular to the (X, Y)-plane.

For $m \ll 1$, the linear approximation is valid for at least propagation distances of the order of a period for most orbits in the reduce phase space, so for large phase mismatch the linear approximation will be sufficient for distances of order $\pi/\Delta k$. Notice that secular terms enter at the next order in this expansion since the amplitude dependence of the period is ignored. This amplitude dependence or Stokes shift of the period is obtained using a multiple time scales or averaging approach.

The leading-order oscillation in Z can also be obtained from the explicit solution for Z in (19). Let $a = (\zeta_1 - \zeta_2)/2$. Then $M = 2a/(\zeta_2 - \zeta_3)$ and as the amplitude of the oscillation in Z tends to zero, $a \to 0$, $M \to 0$, and $Z \to \zeta_2 - a(1 - \cos[k(\xi - \xi_0)]) + O(a^2)$, where $k = ((\zeta_1 - \zeta_3)/2)^{1/2}$. In this limit the period is $2\pi/k$. The correction the period due nonlinear terms is calculated as

$$L = \frac{\pi}{k}\left[1 + \left(\frac{1}{2}\right)^{1/2} M + \ldots\right] \tag{25}$$

by expanding the expression (20) for L in the small amplitude limit.

5. CONTROL VISUALIZED ON THREE-WAVE SURFACES

In this section we analyze the control of energy flow among the three light waves. In previous work[5] a potential equation analogous to (15) was solved directly in (ρ, ϕ) coordinates and quasi-phase-matching was analyzed using the solutions. These solutions can be

visualized either by considering deformations of the potential $U(Z)$ or the phase portrait in $(Z, dZ/d\xi)$ as the values of the parameters s and $\Delta\Gamma$ are varied. Here we use the phase space on the three-wave surface to visualize the transfer of energy among the three light waves. In this setting the phase portrait deforms in a simple way as the parameters s and $\Delta\Gamma$ vary, and it is easy to see how to manipulate the dynamics of the three-wave interaction.

On the reduced three-wave surface information about all three wave-amplitudes as well as the relative phase is retained. As noted above, only information about the absolute phases was removed during the process of symmetry reduction.

Controlling the transfer of energy among the light waves can be analyzed as a motion planning problem on a three-wave surface. In the three-wave equations (2a)–(2c) either the linear or nonlinear term may play the role of the control vector field. The goal is to move from a point on the three-wave surface associated with the initial state of the three-wave system to a second point associated with maximum conversion. As noted earlier, one way to do this is to vary the phase matching parameter until the initial point is connected to the final point with a single orbit. In practice this is achieved by temperature or angle tuning the crystal to phase match the waves. This procedure is often difficult to implement in devices and reduces their robustness.

When the system is not perfectly phase matched, an initial point on the three-wave surface can still be connected to any final point by modulating the material parameters. For instance, if the phase space velocities for $s = 1$ and $s = -1$ are independent at each point of the three-wave surface, then the reduced system is controllable; any pair of points can be joined by a finite concatenation of $s = 1$ and $s = -1$ flows. As the parameters are modulated a point on the three-wave surface is first pushed in one direction and then in another. In this way any point on the three-wave surface can be reached in finite time and the three-wave system can be controlled up to the value of the absolute phases.

When the reduced phase portraits associated with the two different choices of material parameters share a fixed point, the system is no longer controllable. In the three-wave system, such an exceptional point appears when $K_2 = K_3$. This is also the case of type-I second harmonic generation. Here both vector fields approach the fixed point along a homoclinic orbit. Even in this special but important case it is possible to get as close in finite time as needed in optical devices. What is more, for large phase mismatch the region of the phase space that is affected is small. Thus the basic requirement to achieve control is that the modulated parameter or parameters produce at least two different directions for

the phase-space velocity vectors at nearly all points on the three-wave surface.

These basic ideas allow a complete understanding of the control of frequency conversion in the fully nonlinear regime and are based on a very simple geometric construction that permits all the basic features to be visualized. We consider two specific cases below.

A. QUASI-PHASE-MATCHING

Quasi-phase-matching is a robust and efficient way to enhance the effective conversion efficiency of optical materials, and it has a simple geometric interpretation. Quasi-phase-matching is achieved by alternating the sign of $\chi^{(2)}$ at every half-period of the oscillation cycle (*i.e.,* the coherence length $l_c = \pi/\Delta k$), which for small m was seen above to be half the linear oscillation period or nearly half a trip around the three-wave surface. Just as conversion from the pump saturates and begins to reverse, the sign of $\chi^{(2)}$ is inverted. This reverses the direction of the conversion process so that more conversion from the pump can take place.

To understand quasi-phase-matching geometrically notice that the transformation $\gamma_j \to -\gamma_j$ or $s \to -s$ leaves the three-wave surfaces invariant but reverses the sign of m and therefore the slope of the Hamiltonian planes. This leads to the following geometrical construction for quasi-phase-matching trajectories: they are obtained by concatenating intersections of the three-wave surface with Hamiltonian planes of alternating slope. In the optimal case, the sign changes along $Y = 0$, at a point of maximal Z on one segment and minimal Z on the next.

In Fig. 4 a quasi-phase-matched trajectory corresponding to type-II second harmonic generation or parametric conversion is plotted on a three-wave surface. It was generated numerically from Eqs. (2a)–(2c) by alternating the sign of the s after steps of size l_c. It spirals down the three-wave surface towards larger values of Z as more light is converted to the second harmonic. A similar picture is obtained in the case of type-I second harmonic generation and is plotted in Fig. 5. Here the second harmonic grows as the trajectory spirals

down the three-wave surface.

To produce maximum conversion, the initial data are chosen in the plane $Y = 0$ where $\Omega = n\pi$ with $n = 0, 2, 4, \ldots$ if $m > 0$ and $n = 1, 3, 5, \ldots$ if $m < 0$. At these points Z has its minimum value and makes the maximum excursion in Z on a given orbit over a half-period. The composite quasi-phase-matching trajectory is constructed as before, changing the sign of the quadratic coefficients each time the plane $Y = 0$ is crossed. In a system where the second harmonic starts from noise, waves initially near the optimum relative phase grow most efficiently. In systems where the signal is seeded, the relative phase is tuned to achieve optimum conversion.[19] If m is small the optimum conversion efficiency is closely approximated by taking steps of length l_c. Even for moderately large values of the slope m conversion is improved because the period depends weakly on the value of $\Delta\Gamma$.

Looking back at (24a)–(24c) we see that for $m \ll 1$ modulating s introduces the dynamics of a driven harmonic oscillator. Thus, periodically poling the quadratic coefficient introduces a periodic driving force. If its period is half the period of the oscillation, parametric instability occurs. This process eventually saturates. One way that this occurs is through the Stokes shift. In Fig. 4 dots are plotted at the points where the poling takes place. Notice that these points do not all lie along $Y = 0$. The error is due to the Stokes shift. The value of this shift is given approximately in (25).

This saturation process is particularly clear as m increases and the linear period becomes an increasingly poor approximation to the actual oscillation period. In this limit quasi-phase-matching conversion saturates after only a few steps of length l_c. At these larger values of m, the signs of the quadratic coefficients must be alternated at half the *nonlinear* period to obtain the most efficient quasi-phase-matching conversion. Because this period varies as the harmonic grows, optimizing the conversion efficiency requires that the length of the poled segments be varied along the propagation path. If m is large enough, only a few layers are needed to produce complete conversion. If the length of the poled segments cannot be varied, corrections to both l_c and the initial relative phase give the constrained optimum conversion efficiency for the system.[5]

B. ZIG-ZAG CONTROL

The usual strategy for quasi-phase-matching described above is only one of many possibilities for controlling energy flow in resonant wave interactions. Any two points on the three-wave surface can be connected by a composite trajectory if the system parameters are modulated between at least two states. In standard quasi-phase-matching the two states are the two signs of $\chi^{(2)}$. An alternate strategy for the robust control of frequency conversion at any value of m works by modulating the sign of the mismatch parameter at a period shorter than the oscillation period for frequency conversion. The portions of the trajectories that are most nearly vertical produce the most conversion and are located near $X = 0$. Therefore, in contrast to the standard quasi-phase-matching strategy, the optimum initial data has relative phase near $\Omega = n\pi/2$, $n = 1, 2, 3 \ldots$. Geometrically, the composite trajectory looks like a zig-zag stepping up the side of the three-wave surface along $X = 0$. A composite zig-zag trajectory is plotted on a three-wave surface in Fig. 6. It moves down the three-wave surface as more light is converted. We refer to this strategy as the zig-zag control.

6. CONCLUSION

A geometric description of frequency conversion in materials with quadratic nonlinearity has been introduced that enables the dynamics of the amplitudes and the relative phase of the waves to be viewed on a single closed surface in three-dimensions. Composite trajectories constructed in the spirit of quasi-phase-matching connect any two points on a three-wave surface as long as the tangent vectors of at least two families of trajectories are not parallel for most points on the reduced surface. Using this approach controls for the three-wave dynamics were analyzed, and both the zig-zag and the well-known quasi-phase-matching strategies were described geometrically.

While a relatively small amount of conversion is obtained between each modulation of the parameters, the net conversion can be quite large, so the average trajectory is approximately

given by a system with a much smaller value of the ratio of mismatch to nonlinearity. In this way controlling the dynamics of the three-wave interaction enhances the net nonlinear response of the material.

Randomly distributed errors in the poling period degrade the conversion efficiency,[5,15] but do not introduce catastrophic errors. This robustness to errors in the poling period is easy to understand using the geometric description of quasi-phase-matching on the three-wave surface. The structure of Eqns. (13a)–(13c) also illustrates important features of frequency conversion that make quasi-phase-matching particularly robust.

The geometric approach for analyzing wave interactions and their control described here provides a general approach that can be used for many other systems. It underscores the idea that engineering the dynamics of wave interactions improves the net performance of optical materials.

Acknowledgements. MSA was partially supported by NSF grants DMS 9626672 and 9508711. GGL gratefully acknowledges support from BRIMS, Hewlett-Packard Labs and from NSF under grants DMS 9626672 and 9508711. JEM was partially supported by the California Institute of Technology and NSF grant DMS-9802106. JMR was partially supported by NSF grant DMS 9508711, NATO grant CRG 950897 and by the Department of Mathematics and the Center for Applied Mathematics, University of Notre Dame.

REFERENCES

1. A. Yariv, *Quantum Electronics* (Wiley, New York, 1980).

2. R. Boyd, *Nonlinear Optics* (Wiley, New York, 1988).

3. A.C. Newell and J.V. Moloney, *Nonlinear Optics* (Addison-Wesley, Redwood City, 1992).

4. J. A. Armstrong, N. Bloembergen, J. Ducuing, and P. S. Pershan, "Interactions between light waves in a nonlinear dielectric," Phys. Rev. **127,** 1918–1939 (1962).

5. K. C. Rustagi, S. C. Mehendale, and S. Menakshi, "Optical frequency conversion in quasi-phase-matched stacks of nonlinear crystals," IEEE J. Quantum Electron. **QE-18,** 1029 (1982).

6. C. J. McKinstrie and G. G. Luther, "Solitary-wave solutions of the generalised three-wave and four-wave equations," Phys. Lett. A **127,** 14 (1988).

7. S. Trillo, S. Wabnitz, R. Chisari, and G. Cappellini, "Two-wave mixing in a quadratic nonlinear medium: bifurcations, spatial instabilities, and chaos," Opt. Lett. **17,** 637 (1992).

8. C. J. McKinstrie and X. D. Cao, "Nonlinear detuning of three-wave interactions," J. Opt. Soc. Am. B **10,** 898–912 (1993).

9. J. Marsden and T. Ratiu, *Introduction to Mechanics and Symmetry*, Vol. 17 of *Texts in Applied Mathematics*, second edition ed. (Springer-Verlag, New York, 1999).

10. M. S. Alber, G. G. Luther, J. E. Marsden, and J. M. Robbins, "Geometric phases, reduction and Lie-Poisson structure for the resonant three-wave interaction," Physica D **123,** 271–290 (1998).

11. M. S. Alber, G. G. Luther, J. E. Marsden, and J. M. Robbins, in *Proceedings of the Fields Institute Conference in Honour of the 60th Birthday of Vladimir I. Arnol'd*,

Fields Institute Communications Series, Field Institute, E. Bierstone, B. Khesin, A. Khovanskii, and J. Marsden, eds., (1999).

12. M. Born and E. Wolf, *Principles of Optics* (Pergamon press, Oxford, 1980).

13. D. David, D. D. Holm, and M. V. Tratnik, "Integrable and chaotic polarization dynamics in nonlinear optical beams," Physics Lett. A 137 (1989).

14. N. N. Akhmediev and A. Ankiewicz, *Solitons* (Chapman & Hall, London, 1997).

15. M. M. Fejer, G. A. Magel, D. H. Jundt, and R. L. Byer, "Quasi-phase-matched second harmonic generation: tuning and tolerances," IEEE J. Quantum Electron. **28,** 2631–2654 (1992).

16. L. E. Myers, R. C. Eckardt, M. M. Fejer, R. L. Byer, W. R. Bosenberg, and J. W. Pierce, "Quasi-Phase-Matched Optical Parametric Oscillators in Bulk Periodically Poled $LiNbO_3$," J. Opt. Soc. Am. B **12,** 2102–2116 (1995).

17. A. Kobyakov, U. Peschel, and F. Lederer, "Vectorial type-II interaction in cascaded quadratic nonlinearities – an analytical approach," Opt. Comm. **124,** 184–194 (1996).

18. A. Kobyakov and F. Lederer, "Cascading of quadratic nonlinearities: a comprehensive analytical study," Phys. Rev. A **54,** 3455–3471 (1996).

19. C. J. Mckinstrie, G. G. Luther, and S. H. Batha, "Signal Enhancement in Collinear 4-Wave Mixing," J. Opt. Soc. Am. B **7,** 340–344 (1990).

Fig. 1. An orbit of the reduced three-wave equations is constructed by intersecting a three-wave surface with a plane that is one level set of the reduced Hamiltonian. Here $p = (-1, -1, 1)$, $s = 1$, $\Delta\Gamma = 40$, and the Manley-Rowe relations are defined by $(q_1(0), q_2(0), q_3(0)) = (0.1, 0.6, 1.0)$.

Fig. 2. A reduced three-wave phase space for type-II second harmonic generation or parametric frequency conversion on a three-wave surface. Here, $p = (-1, -1, 1)$, $s = 1$, $\Delta\Gamma = 10$, and the Manley-Rowe relations are defined by $(q_1(0), q_2(0), q_3(0)) = (1.0, 0.5, 2.0)$.

Fig. 3. A reduced three-wave phase space for type-I second harmonic generation on a three-wave surface, where $p = (-1, -1, 1)$, $s = 1$, and $\Delta\Gamma = 2$. The Manley-Rowe relations are defined by $(q_1(0), q_2(0), q_3(0)) = (1.0, 1.0, 2.0)$, so $K_2 = K_3$.

Fig. 4. A composite trajectory with 30 segments of length $l_c = \pi/\Delta k$ for type-II quasi-phase-matching or parametric frequency conversion is plotted on a three-wave surface. Here $p = (-1, 1, 1)$, $\Delta\Gamma = 40$, and initially $s = 1$ and $(q_1(0), q_2(0), q_3(0)) = (0.0, 1.0, 1.0)$.

Fig. 5. A composite trajectory with 30 segments of length $l_c = \pi/\Delta k$ for type-I quasi-phase-matching second harmonic generation. Here $p = (1, 1, -1)$, $\Delta\Gamma = 40$, and initially $s = 1$, and $(q_1(0), q_2(0), q_3(0)) = (1.0, 1.0, 0.0)$.

Fig. 6. A composite trajectory for the zig zag strategy for type-II second harmonic generation. The phase mismatch is modulated after $l_c = \pi/(2\Delta k)$ and $(q_1(0), q_2(0), q_3(0)) = (0.1, 0.6, \exp(i * \pi/5))$, so the initial relative phase is near $\pi/5$. Here $s = 1$, $\Delta\Gamma = 10$, and the Z coordinate is defined by $p = (-1, -1, 1)$.

Fig. 1

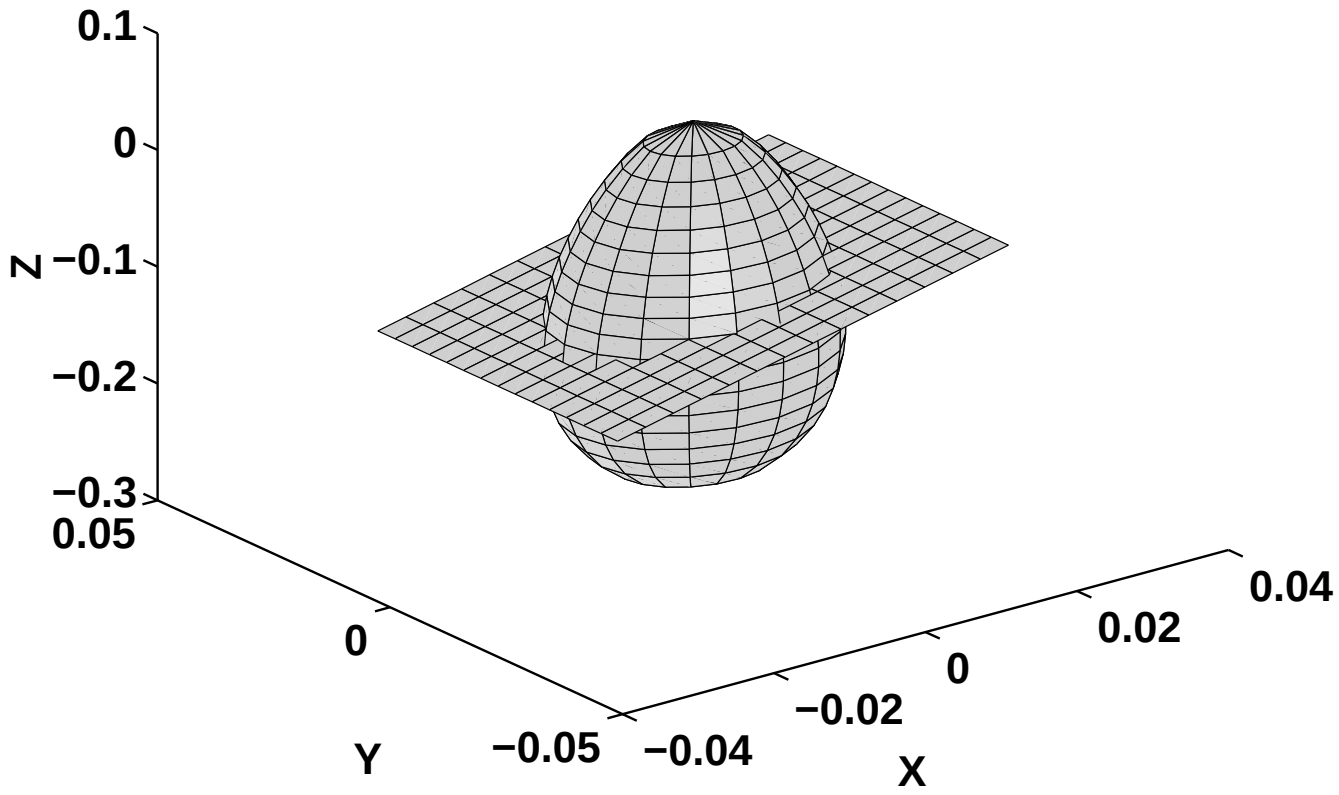

Fig. 2

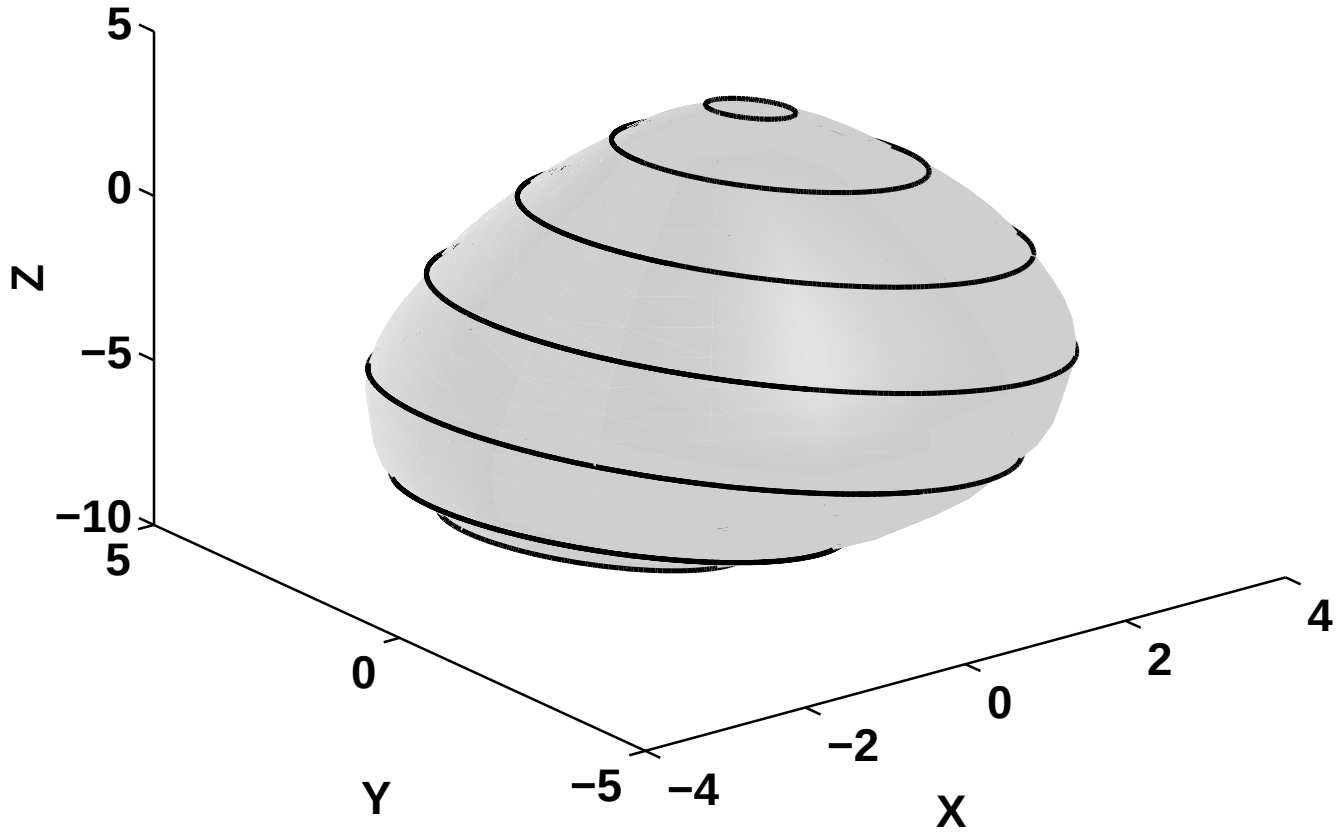

Fig. 3

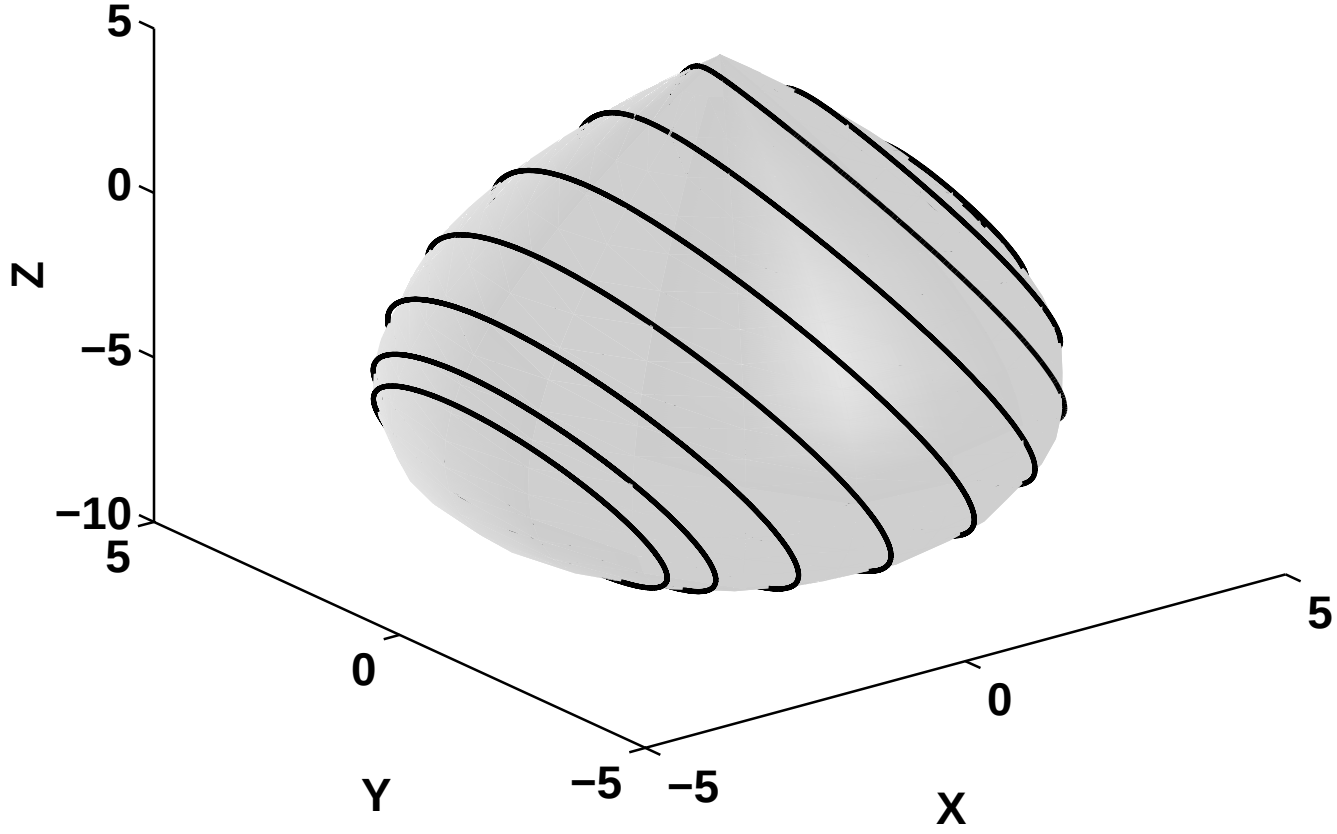

Fig. 4

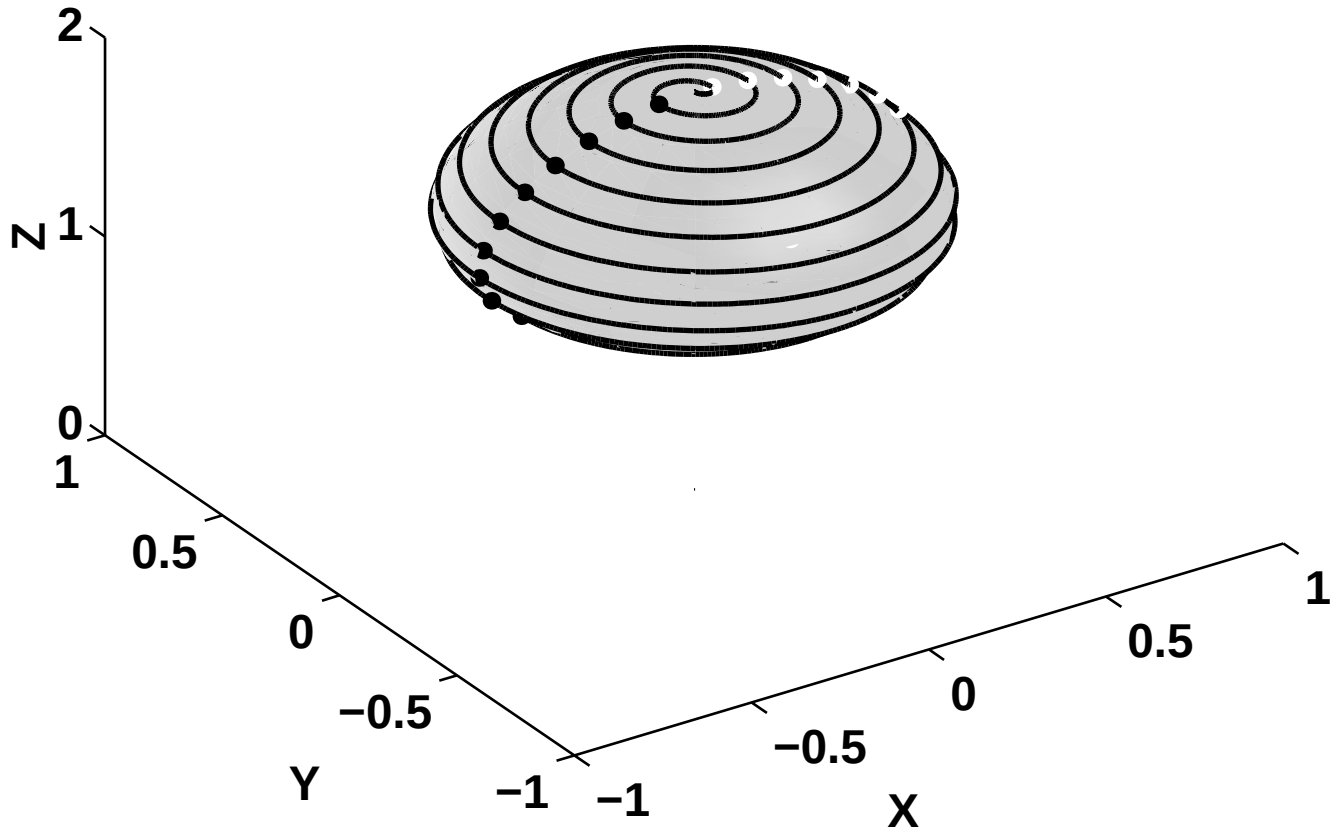

Fig. 5

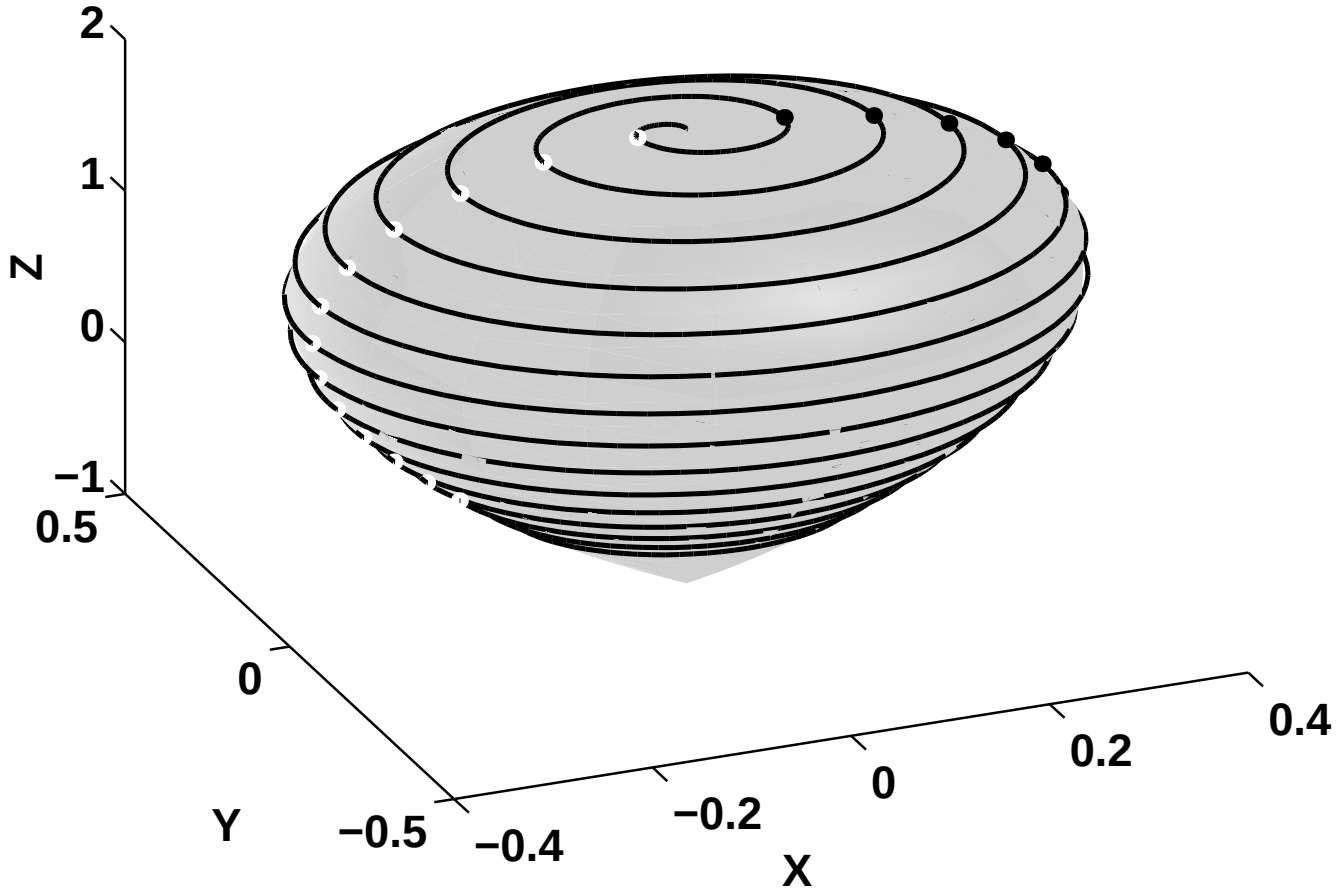
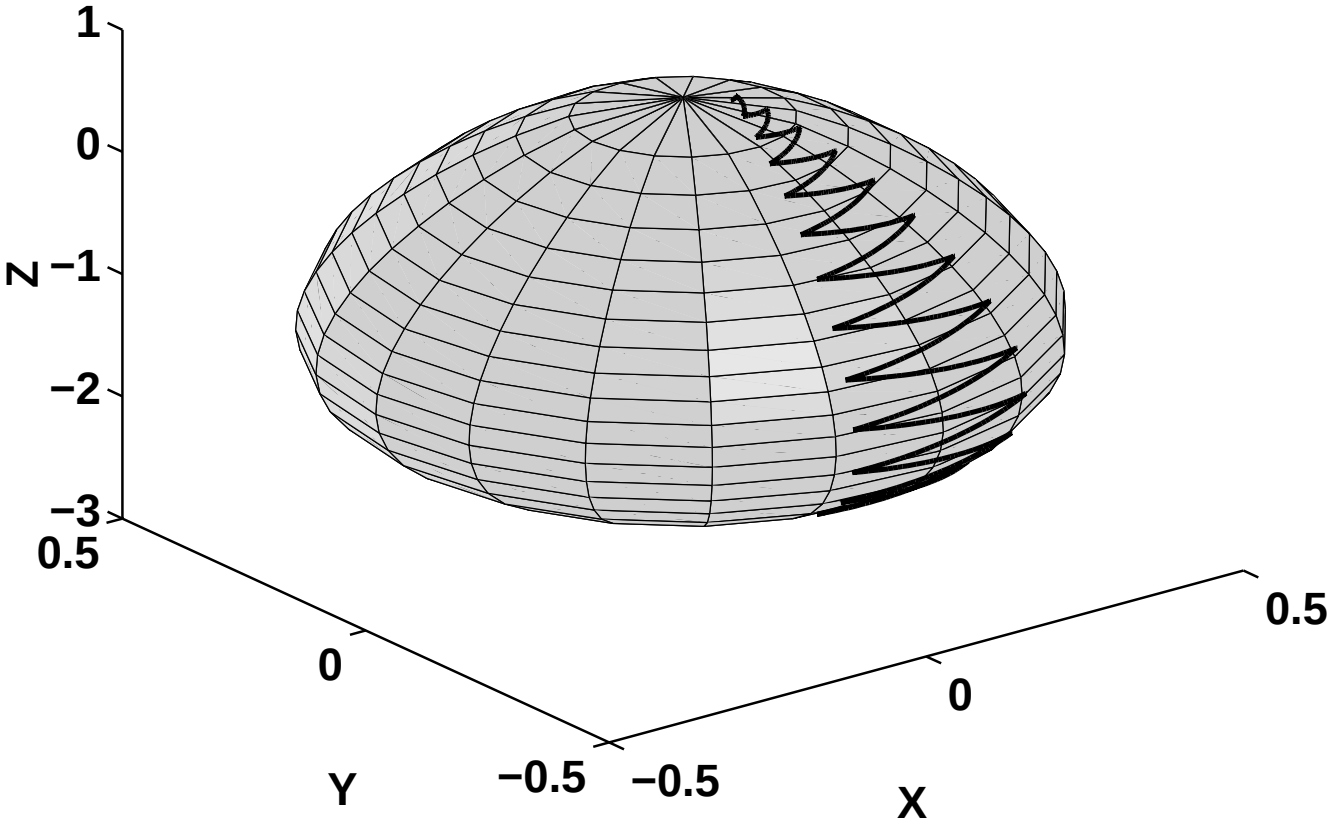
Fig. 6